FULL PAPER

Dalton
www.rsc.org/dalton

Engineering cytochrome P450cam into an alkane hydroxylase

Stephen G. Bell, Erica Orton, Helen Boyd, Julie-Anne Stevenson, Austin Riddle, Sophie Campbell and Luet-Lok Wong*

Department of Chemistry, Inorganic Chemistry Laboratory, University of Oxford, South Parks Road, Oxford, UK OX1 3QR

Received 22nd January 2003, Accepted 26th March 2003
First published as an Advance Article on the web 9th April 2003

The haem monooxygenase cytochrome P450cam from *Pseudomonas putida* has been engineered into an alkane hydroxylase. Active site amino acid residues were substituted with residues that have bulkier and more hydrophobic side-chains. The residues F87, Y96, V247 and V396, which are further away from the haem, were targeted first for substitution in order to constrain the small alkanes *n*-butane and propane to bind closer to the haem. We found that just two mutations could increase the alkane oxidation activity of P450cam by two orders of magnitude. The F87W/Y96F/V247L triple mutant was then used as a basis for introducing further substitutions, at the residues T101, L244, V395 and D297 which are closer to the haem, to improve the enzyme/alkane fit and hence the alkane hydroxylase activity. The F87W/Y96F/T101L/V247L mutant oxidised *n*-butane with a catalytic turnover rate of 755 nmol(nmol P450cam)$^{-1}$(min)$^{-1}$, which is comparable to the camphor oxidation activity of the wild-type (1000 min^{-1}). The F87W/Y96F/T101L/L244M/V247L mutant had lower *n*-butane oxidation activity but the highest propane oxidation rate (176 min^{-1}) of the P450cam enzymes studied. All P450cam enzymes gave 2-butanol and 2-propanol as the only products. Determination of the extent of uncoupling showed that hydrogen peroxide generation was the dominant uncoupling mechanism. The data indicate that further mutations at residues higher up in the active site are required to localise the substrates close to the haem and to reduce substrate mobility. These next-generation mutants will have higher activity, and may be able to catalyse the oxidation of ethane and methane.

Introduction

The cytochrome P450 (CYP) enzymes are haem dependent monooxygenases that primarily catalyse the oxidation of C–H bonds to the alcohol functionality. P450 enzymes are known to oxidise a very extensive range of endogenous and exogenous organic compounds, ranging from medium chain alkanes such as *n*-heptane and *n*-octane, to steroidal and polyaromatic compounds, and very large molecules such as the triterpenes and cyclosporin.[1,2] These reactions are important in biological systems because they are crucial steps in biosynthesis, cellular biochemistry, metabolism, pharmacology and medicine. There has been much effort directed at understanding the relationship between P450 structure, function and reactivity.[2] P450 enzymes follow a common mechanism,[3] in which a reactive intermediate generated during the catalytic cycle attacks a C–H bond in a substrate bound close to the haem iron. The nature of this C–H bond activating intermediate remains controversial, but the consensus is for an oxyferryl porphyrin radical cation species.[4] Since the formation of this ferryl intermediate does not depend on the stabilisation of a transition state involving the substrate, the substrate specificity of P450 enzymes depends on what substrate can enter and bind within the active site. The orientation in which the substrate is bound, then determines which group is closest to the reactive intermediate for attack, and hence the products formed.

The unique C–H bond activation activity of cytochrome P450 enzymes have no equivalents in classical synthetic methodologies, and so these enzymes have many potential applications in biotransformation.[5–7] Research efforts in this area have focussed on the soluble bacterial enzymes, in particular the structurally characterised P450cam from *Pseudomonas putida* [3,8] and P450BM-3 from *Bacillus megaterium*.[9–11] The selective catalytic oxidation of alkanes to alcohols without further oxidation to the aldehydes or ketones, is a major target of catalysis research. An efficient process for the oxidation of methane to methanol, ethane to ethanol, and of the higher homologues, especially to the terminal alcohols, will have very significant impact on industrial processes by providing new feedstocks for the synthesis of complex molecules. All current industrial alkane oxidation processes utilise metal oxide catalysts operating at elevated temperatures and pressures, while homogeneous catalysts do not yet have the required activity, selectivity or catalyst lifetime.

Numerous microorganisms are known to oxidise alkanes as part of their metabolic or catabolic pathways, and indeed some can grow on the chemically inert alkanes as the sole carbon and energy source. Many alkane metabolising yeast strains use P450 enzymes to activate alkanes such as *n*-octane; the most well characterised is the CYP52 enzyme from *Candida maltosa*.[12] Alkane hydroxylase is a non-haem iron enzyme from *Pseudomonas oleovorans* that oxidises linear alkanes to the terminal alcohols.[13–15] The most spectacular are the methane-oxidising bacteria such as *Methylococcus capsulatus* (Bath)[16–19] and *Methylosinus trichosporium* Ob3b,[20–22] which grow on methane by using methane monooxygenases (MMO) to activate the highly inert methane C–H bond. MMO can also oxidise longer chain alkanes, although further oxidation of the initial alcohol products is a potential problem. The P450 enzymes have also been investigated for alkane oxidation. We have described the engineering of P450cam for the oxidation of the short chain alkanes butane, pentane and hexane.[23–25] Forced evolution of P450BM-3 has generated a mutant with 13 mutations, none of which was within the active site, that oxidised *n*-octane with the very high NADPH turnover rate of 8000 min^{-1}, and *n*-butane (1830 min^{-1}) and propane (850 min^{-1}) are also oxidised at fast rates.[26]

We,[27–31] and others,[32–39] have shown that P450cam can be engineered to oxidise many different classes of compounds that are structurally unrelated to the natural substrate, camphor. We report here the results our recent efforts to engineer P450cam into an alkane hydroxylase, with particular emphasis on the oxidation of the smaller, gaseous alkanes. We have previously shown that increasing the hydrophobicity of the active site with the Y96A and Y96F mutations promoted the oxidation of alkanes,[23] and that decreasing the active site volume favoured the oxidation of less sterically demanding alkanes.[24] For instance the Y96F/V247L mutant oxidised hexane at a faster rate than 3-methylpentane while the Y96A/V247L mutant showed the opposite activity trend. Our approach was therefore to decrease the active site volume by targeting residues in the P450cam substrate-binding pocket for substitutions with amino

DOI: 10.1039/b300869j

acids with bulkier side-chains, in order to promote the binding and oxidation of the small alkane molecules.

Materials and methods

General

Enzymes for the molecular biology work were from New England Biolabs, UK. Buffer components were from Anachem, UK. The alkane substrates, the alcohol products, and general reagents were from Sigma/Aldrich or Lancaster, UK. NADH was from Roche Diagnostics, UK. UV/Vis spectra were recorded on a Varian CARY 1E double-beam spectrophotometer equipped with a Peltier cell temperature controller (± 0.1 °C). Gas chromatography analyses were performed on a Fisons Instruments 8000 series gas chromatograph equipped with a flame ionisation detector (FID). The *n*-pentane oxidation products were analysed on a DB-1 fused silica column (0.25 mm i.d. × 30 m) or a β-DEX chiral phase column (0.25 mm i.d. × 30 m), while a SPB-1 column (0.5 mm i.d. × 60 m) together with a special injector liner was used for the lighter alcohols: the butanols, the propanols, ethanol and methanol.

Enzymes and molecular biology

General DNA and microbiological manipulations were carried out by standard methods.[40] The P450cam enzyme and the physiological electron transfer co-factor proteins putidaredoxin and putidaredoxin reductase, were expressed in *Escherichia coli* and purified as previously described.[41–43] The proteins were readily purified by anion exchange chromatography and were stored at −20 °C in buffers containing 50% v/v glycerol as cryoprotectant. The glycerol was removed from the proteins immediately prior to activity assays by gel filtration on a 5-mL bed volume PD-10 column (Amersham Biosciences, UK), eluting with 50 mM Tris, pH 7.4. Site-directed mutagenesis was carried out by a polymerase chain reaction (PCR)-based method using the QuikChange kit from Stratagene using oligonucleotides designed following the manufacturer's guidelines. For example the oligonucleotide 5′-TACGACTTCATTCC-CCTCTCGATGGATCCGCC-3′, and its reverse complement, were used to introduce the Thr101 ⟶ Leu (T101L) mutation (the codon for residue 101 is underlined). Oligonucleotides for site-directed mutagenesis were from MWG-Biotech. New mutants were identified and then fully sequenced by automated DNA sequencing on an ABI 377XL Prism DNA sequencer by the DNA sequencing facility at the Department of Biochemistry, University of Oxford. All P450cam enzymes described in this work also contained the Cys334 ⟶ Ala (C334A) base mutation which prevents protein dimerization *via* disulfide bond formation.[44] For convenience, the C334A base mutant is referred to as 'wild-type', and the Y96F/C334A double mutant as Y96F, *etc*. The Y96F, F87W/Y96F, Y96F/V247L and F87W/Y96F/V247L mutants had been reported previously.[30]

NADH turnover rate determinations

All incubations were carried out at 30 °C. Incubation mixtures contained 50 mM Tris, pH 7.4, 200 mM KCl, 1 μM P450cam, 10 μM putidaredoxin, 1 μM putidaredoxin reductase, and 30 μg mL^{-1} bovine liver catalase,[23] except where the extent of uncoupling to form hydrogen peroxide was to be determined. The mixtures were oxygenated and then equilibrated at 30 °C for 2 min. For *n*-pentane oxidation reactions (final incubation volume 1.7 mL), the substrate was added as a 10 mM stock in ethanol to a nominal final concentration of 500 μM. NADH was added as a 20 mg mL^{-1} stock solution in 50 mM Tris, pH 7.4, to *ca*. 400 μM (final A_{340} = 2.5) and the absorbance at 340 nm was monitored. The rate of NADH consumption was calculated from the slope of the time-course plot using ε_{340} = 6.22 mM^{-1} cm^{-1}. The maximum concentration of ethanol in an incubation reaction was <1% v/v, and control experiments showed that ethanol on its own at up to 10% v/v did not induce any increase in the rate of NADH consumption.

Incubations with the gaseous alkanes *n*-butane, propane, ethane and methane were carried out in 4-mL capacity cuvettes equipped with a screw cap and Teflon septum seal. The final volume of incubations was 2.5 mL. The concentration of the reaction components was the same as those for reactions with *n*-pentane. In a typical reaction the volume of buffer required to take the final volume to 2.5 mL was *ca*. 1.6 mL. Half of this required volume of buffer was saturated with the gaseous alkane substrate, while the other half was a buffer solution saturated with oxygen. The cuvette was immediately sealed with the Teflon-backed screw cap and the reaction was initiated by the addition of NADH *via* a hypodermic syringe needle pushed through the Teflon septum.

For many mutant/*n*-butane, and some mutant/propane combinations it was necessary to reduce the concentration of NADH to initiate the reaction because the coupling efficiencies were so high that the alkane substrate was fully consumed. In these cases only 200 μM of NADH was added so as to maintain the substrate in excess and to keep the P450cam enzyme saturated with substrate. Interestingly even when the *n*-butane or propane were exhausted in incubations, there was no further oxidation of the 2-butanol or 2-propanol to the ketones.

Assays for the alkane oxidation products

After all the NADH had been consumed in an incubation, 3-methyl-2-pentanol was added as an ethanol stock to the *n*-pentane oxidation reactions to act as an internal standard (final concentration 300 μM) for the solid phase extraction and GC analysis steps. Organics in a 1-mL aliquot of the incubation mixtures were adsorbed onto a Varian Bond-Elut C_{18} column (1 mL matrix volume) which had been equilibrated by washing with 1 mL methanol followed by 1 mL 50 mM Tris, pH 7.4. The column was then washed with 1 mL 50 mM Tris, pH 7.4, and dried under vacuum for 5 min. Bound organics were eluted with 300 μL chloroform and then analysed by GC on the DB-1 column. The injector temperature was 120 °C and the FID was held at 250 °C. The temperature of the DB-1 column was maintained at 40 °C. Under these conditions 2-pentanol and 3-pentanol were eluted as one peak at 3.89 min. Further analysis with a β-DEX chiral phase column (temperature profile: 40 °C for 1 min then 3 °C per min to 100 °C and then maintained at 100 °C for 8 min) showed that all the P450cam enzymes gave virtually statistical mixtures (2-pentanol : 3-pentanol ≈ 2 : 1) of these compounds, with small amounts (<2% total) of 2-pentanone and 3-pentanone also detected.

The concentration of the pentanol products in incubation mixtures was determined by calibrating the concentration response of the FID to 2-pentanol. Mixtures containing different concentrations of 2-pentanol and all the components of a normal incubation, except NADH and substrate, were extracted and analysed as for normal incubations. Control analyses showed that, as expected, the FID response to the isomeric 2-pentanol and 3-pentanol were identical, within experimental error. The plot of the ratio of the 2-pentanol peak area to the internal standard, against the 2-pentanol concentration, gave a straight line passing through the origin. The absolute quantity of pentanol products formed by enzymatic turnover in an incubation mixture was then readily determined. The coupling efficiency was the percentage of NADH consumed that led to product formation. Control experiments showed that the solid phase extraction procedure gave highly reproducible results, with <5% variation across a large number of analyses.

For the lighter alcohols formed by the oxidation of gaseous alkanes, the solid phase extraction method was less reliable and

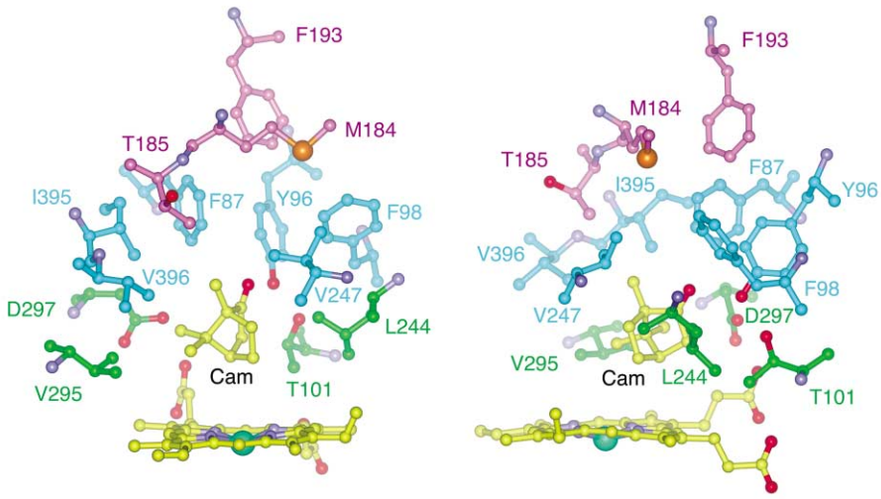

Fig. 1 The active site structure of wild-type cytochrome P450cam with bound camphor. Both figures are views from the side, with depth cue, to show the Tier-like arrangement of active site residues and the location of the residues. Side-chains of residues in the separate Tiers are coloured differently – Tier 1: green, Tier 2: cyan, Tier 3: purple. The backbone nitrogen is coloured blue, and the backbone carbonyl oxygen is omitted for clarity. The camphor carbonyl group forms a hydrogen bond with the phenolic side-chain of Tyr-96. There are complementary van der Waals contacts between camphor and the side-chains of Phe-87, Thr-185, Leu-244, Val-247 and Val-295. The figures were generated with the program WebLab Viewer from the entry 2cpp from the Protein Data Bank.

in fact not suitable for ethanol and methanol. Extraction with organic solvents was not satisfactory because of the poor partition of methanol, ethanol and the propanols into the organic phase. In addition even contamination of the solvents by <0.1% v/v of the lighter alcohols became an issue. Furthermore the DB-1 column could not resolve 2-propanol from most of the common organic solvents. We therefore used a SPB-1 column (0.5 mm i.d. × 60 m) for the analysis of these alcohols. The SPB-1 column also had the added advantage of being tolerant of water and thus allowed the direct injection of incubation mixtures for GC analysis. However, this required a special injector liner because the normal straight glass tube liners did not give clean and consistent vaporisation of water which has the tendency to shatter into microscopic droplets upon initial contact with the hot surface. This "beading" of water normally results in broad and poorly resolved peaks. With the special liner we were able to obtain well-defined peaks consistently.

For the analysis of aqueous reaction samples, 90 μL of the reaction mixture was added to a 10-μL aliquot of a 200 μM solution of 1-pentanol in water; the 1-pentanol acting as the internal standard. A 2-μL aliquot of such a mixture was injected directly onto the column. The oven temperature was held at 40 °C for 4 min and then increased at 5 °C min^{-1} to 100 °C, and held at 100 °C for 2 min. The retention times were: methanol 2.8 min, ethanol 3.5 min, 2-propanol 4.8 min, 2-butanol 8.5 min, and 1-pentanol (internal standard) 16.0 min. All the P450cam enzymes studied in this work oxidised *n*-butane to 2-butanol only, and 2-propanol was the only product from propane.

Uncoupling *via* hydrogen peroxide formation

The extent of uncoupling of NADH consumption to hydrogen peroxide generation was determined for *n*-butane and propane oxidation by a standard assay using phenol, 4-aminoantipyrine and horseradish peroxidase. The concentration of the quinone-imine product formed was determined from the absorbance at 500 nm by using $\varepsilon_{500} = 6850\ M^{-1}\ cm^{-1}$.

Results and discussion

Engineering P450cam for alkane oxidation

We adopted the approach of searching for a P450cam mutant with high activity for the oxidation of a longer chain alkane such as *n*-pentane and then to seek additional mutations that will promote the oxidation of *n*-butane and propane. Since the alkane substrates are smaller than camphor, active site substitutions were made with amino acids such as leucine, methionine, phenylalanine and tryptophan, which have larger side-chains. The expectation was that, as additional mutations were introduced, the volume of the P450cam active site will be reduced, and the substrate specificity will be increasingly biased towards the smaller, gaseous alkanes.

The structure of wild-type P450cam with bound camphor is shown in Fig. 1.[45] Sligar and coworkers have described this structure as being made up of three Tiers.[3,34] In Tier 1 are the residues T101, L244 and V295, which are close to the haem. The side-chains of F87, Y96, V247, I395 and V396 in Tier 2 almost form a ring above Tier 1, while the side-chain of T185 and, to a lesser extent, M184, cover the top of the active site. Loida and Sligar reported that the V247A (Tier 2) and T101M (Tier 1) mutations reduced the ethylbenzene oxidation activity of P450cam.[34] It was suggested that this arose because the V247A mutation created space in the upper part of the active site to allow the substrate to bind away from the haem, while the T101M mutation restricted the space available close to the haem and thus forced the substrate to bind further away. Amino acid substitutions at the Tier 3 residue T185 had relatively minor effects on the oxidation of a series of alkylbenzene compounds.[34] We reasoned that bulky substitutions at T185 may not be necessary if it proved possible to reduce the space in the upper parts of the P450cam active site by bulky substitutions in Tier 2. This approach has been successfully applied to the protein engineering of P450cam for the reductive dehalogenation of chlorinated ethanes,[3] and the oxidation of alkanes,[23–25] and polychlorinated benzenes.[29,30] After a good combination of mutations in Tier 2 was found, we would introduce additional bulky substitutions in Tier 1 to improve further the alkane oxidation activity.

n-Pentane oxidation activity

The *n*-pentane oxidation activity of the first series of mutants designed to establish a good combination of mutations in the upper part of the P450cam active site are given in Table 1. Bulky amino acid substitutions were carried out at the Tier 2 sites F87, Y96, V247 and V396. In addition the F98W mutation was also introduced. The side-chain of F98 does not form part of the active site but it contacts the side-chain of Y96,

Table 1 The pentane oxidation activity of wild-type and mutants of P450cam. The NADH turnover and the product formation rates are given in nmol per nmol of P450cam per min. The data are means of at least three experiments, with all data for each parameter being within 15% of the mean. n.d.: no product detected

P450cam enzyme	NADH oxidation rate	Product formation rate	Coupling (%)
Wild-Type	6.4	0.07	1.1
Y96F	405	106	29.5
Y96F/V247A	152	31	22
Y96F/V247L	510	227	44.5
Y96F/F98W	32	0.4	1.3
F87W/Y96F	471	192	42.5
F87W/Y96F/F98W	367	26.5	7.2
F87W/Y96F/V247L	510	237	46.5
F87W/Y96W/V247L	64	n.d.	*n.d.*
F87W/Y96F/F98W/V247L	26	1.0	3.8
F87W/Y96F/V247L/V396L	76	1.7	2.3

and substitutions here may influence the alkane oxidation activity.

All the P450cam enzymes studied gave virtually statistical (2 : 1) mixtures of 2-pentanol and 3-pentanol. Some mutants also gave small (<2% in total) amounts of the corresponding pentanones, but 1-pentanol or pentanal were not observed. The radical rebound mechanism generally accepted for P450 catalysis suggests that *n*-pentane is sufficiently mobile within the active site of the P450cam enzymes such that the more reactive secondary C–H bonds are preferentially attacked over the primary C–H bonds at the terminal carbons.

The activity data (Table 1) clearly show that even a small number of active site mutations can greatly increase the alkane oxidation activity of P450cam. For comparison the camphor oxidation activity of wild-type P450cam under identical conditions is 1000 min^{-1}. The largest increase in activity over the wild-type was imparted by the Y96F mutation first described by Atkins and Sligar.[46] The increase was a result of both enhanced NADH oxidation rate and coupling efficiency (the product yield based on NADH consumed). Under the assay conditions the rate-limiting step for the NADH oxidation activity is the first electron transfer from reduced putidaredoxin to the ferric, substrate-bound P450cam. According to the Marcus Theory of electron transfer,[47] this reaction is faster for a higher thermodynamic driving force and lower reorganisation energy. Binding of a substrate sufficiently close to the haem could displace the haem iron sixth ligand, water, leading to an increase in the haem reduction potential and a decrease in the reorganisation energy of electron transfer because the haem in both the ferric and ferrous forms would be five-coordinate.[48] However, these criteria do not restrict the motion of the bound substrate—as long as it is sufficiently close to the haem to cause dissociation of the water ligand, fast electron transfer should ensue. We have suggested previously that the Y96F mutation promotes the binding and oxidation of hydrophobic organic molecules by increasing the active site hydrophobicity and facilitating the displacement of water molecules from the active site.[23] Thus *n*-pentane is bound more strongly and the haem ligand water displaced more readily in the Y96F mutant, leading to faster electron transfer and higher NADH oxidation activity compared to the wild-type enzyme.

Uncoupling of reducing equivalents from the electron donor (NADH or NADPH) away from product formation is a major feature of P450 catalysis, especially in the oxidation of unnatural substrates. For these compounds, it is possible that the NADH consumption activity is very high but the rate of product formation is slow (see Table 1) because most the reducing equivalents are channelled away to form hydrogen peroxide and water.[27] The extent of uncoupling is therefore a stringent measure of the match between the substrate and the enzyme active site than the NADH oxidation rate.[34] A number of uncoupling mechanisms can be envisaged. If the substrate is mobile, a certain population of the enzyme could have a substrate bound too far away from the haem, such that the ferryl intermediate does not undergo rapid attack on the substrate but is instead reduced by the electron transfer co-factor protein back to the ferric resting state. The overall catalytic cycle would then result in the four-electron reduction of dioxygen to two molecules of water, *i.e.* oxidase activity (Fig. 2). Interconversion between different substrate binding orientations could also lead to the transient approach of water molecules into the active site.[49,50] The presence of these water molecules could lead to protonation of the ferric hydroperoxy intermediate at the iron-bound oxygen, resulting in loss of hydrogen peroxide. Extra water molecules in the oxygen binding groove in the kink in the distal I helix, around the T252 side-chain,[45,51] could also interfere with the delivery of protons to the hydroperoxy oxygen atom which is not bound to the haem, again leading to peroxide dissociation. The most stable location of substrate binding may be very close to the haem iron, resulting in steric interaction between the substrate and the bound dioxygen or hydroperoxy ligand. It should be noted that if the bulky substitutions reduced the active site volume by too much, an unnatural substrate such as *n*-pentane might be forced to bind so close to the haem iron that such steric interactions would give rise to uncoupling. Finally, there may be steric hindrance between the substrate and the hydroperoxy ligand during the interconversion between different substrate binding modes. Both these steric effects could weaken the iron–hydroperoxide interaction and lead to the loss of hydrogen peroxide.[49]

The Y96F mutation greatly enhanced the coupling efficiency of *n*-pentane oxidation (29.5%) compared to the wild-type enzyme (1.1%). The major uncoupling pathway for both enzymes was hydrogen peroxide formation, but this pathway was much reduced in the mutant. Since *n*-pentane is smaller than camphor and also very conformationally flexible, the Y96F mutation on its own is not expected to prevent completely the entrance of water molecules to the active site or to confer a unique *n*-pentane binding orientation. Nevertheless the increased active site hydrophobicity in the mutant should facilitate the expulsion of active site water molecules and thus retard the peroxide uncoupling pathway.

Addition of the bulky substitutions F87W or V247L, to the Y96F mutation, doubled the *n*-pentane oxidation activity, mainly by increasing the coupling efficiency, whilst the V247A mutation reduced the activity by 60%. These results are consistent with the proposal that bulky substitutions in Tier 2 should increase the activity and coupling of the oxidation of a small substrate by constraining it to bind close to the haem, while mutations that generate space in the upper part of the pocket should reduce the activity.[34] When the Y96F, F87W and V247L mutations were combined, the Y96F/F87W/V247L mutant did not show significantly higher *n*-pentane oxidation activity than the double mutants, suggesting that there may be competition between the effects of the F87W and V247L mutations.

Some mutations had unexpected effects. The Y96W, F98W and V396L mutations reduced the activity by as much as two orders of magnitude. It is not clear why the V396L mutation

Table 2 The *n*-butane and propane oxidation activity of wild-type and mutants of P450cam. The rates of NADH turnover and the formation of product (2-butanol and 2-propanol) are given in nmol per nmol of P450cam per min. The data are means of at least experiments, with all data for each parameter being within 15% of the mean

	n-Butane			Propane		
P450cam enzyme	NADH oxidation rate	Product formation rate	Coupling (%)	NADH oxidation rate	Product formation rate	Coupling (%)
Wild-Type	8	0.4	0.5	9	0.5	0.5
Y96F	100	42	42	18	2.2	12
F87W/Y96F	200	132	66	60	12	20
Y96F/V247L	250	188	75	110	43	39
F87W/Y96F/V247L	263	89	34	82	14	17
F87W/Y96F/T101L	546	459	85	198	51	26
Y96F/T101L/V247L	423	186	44	152	20	13
F87W/Y96F/T101L/V247L	795	755	95	346	111	32
F87W/Y96F/T101M/V247L	373	205	55	164	66	40
F87W/Y96F/V247L/V295I	363	99	27.5	124	3.5	3.0
F87W/Y96F/V247L/V396L	52	12.5	24	7.5	1.5	18
F87W/Y96F/T101L/V247L/D297M	385	243	63	214	56	26
F87W/Y96F/T101L/V247L/L244M	578	520	90	266	176	66

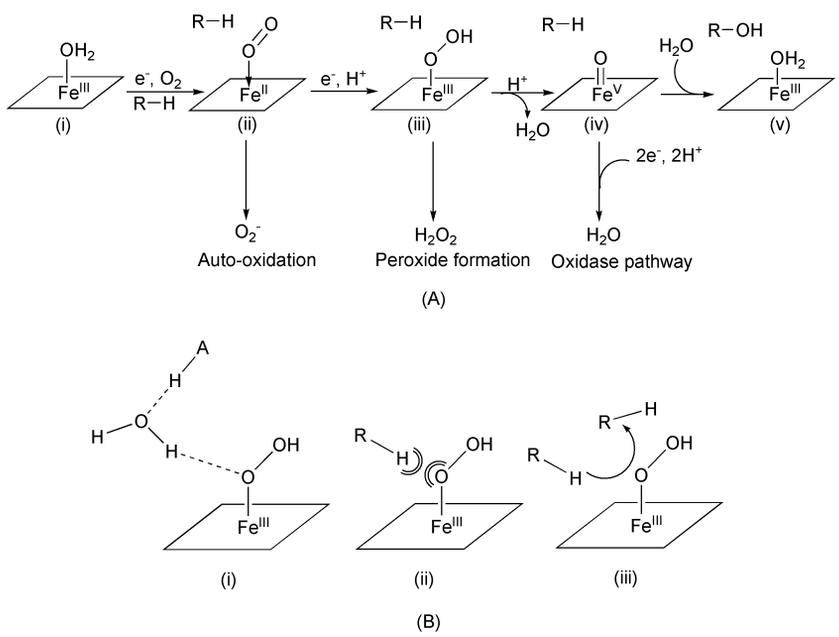

Fig. 2 (A) The catalytic mechanism of cytochrome P450cam showing the three potential uncoupling pathways of auto-oxidation of the ferrous-oxy form (ii), hydrogen peroxide generation and oxidase reactivity. The auto-oxidation pathway is much slower than the other steps and can be ignored in most cases. (B) Three mechanisms of the peroxide uncoupling pathway. In (i) the accessibility of the haem-bound oxygen to water molecules leads to protonation and loss of hydrogen peroxide; this reaction should require the participation of a general acid on the side-chain of a residue. The schematic in (ii) shows the steric hindrance between the hydroperoxy ligand and a substrate that is bound too close to the haem iron which can weaken the Fe^{III}–OOH interaction and cause dissociation of the hydroperoxide anion. In (iii) the possibility of multiple substrate-binding orientations is shown with two R–H substrate molecules. The arrow represents a trajectory of interconversion between different binding orientations which brings the substrate close to the haem-bound hydroperoxy ligand. Steric interactions could again weaken ligand binding, resulting in the loss of the hydroperoxide ion.

reduced the *n*-pentane oxidation activity in the F87W/Y96F/V247L/V396L mutant, although the presence of four such bulky substitutions in Tier 2 might have unpredictable effects such as causing the structure to change and the actives site to open up compared to the wild-type. The detrimental effects of the Y96W mutation on P450cam substrate oxidation activity has been reported.[39] The F98 side-chain is not part of the active site but rather the interior of the protein, although it contacts the side-chain at the 96 position. It is possible that the F98W mutation caused structural changes that reduced the activity. In addition, the Y96 side-chain is proposed to be part of the substrate access channel,[45,52] and so both the Y96W and F98W mutations could also affect substrate entry.

From the results of the initial screening of mutations, the F87W/Y96F/V247L mutant was chosen as the starting mutant for introducing substitutions at Tier 1 residues to promote the oxidation of the smaller, gaseous alkanes.

The oxidation of *n*-butane and propane

Before adding mutations to the F87W/Y96F/V247L triple mutant, we examined the *n*-butane and propane oxidation activity of all the mutants tested for *n*-pentane oxidation. The results for some mutants are given in Table 2. All P450cam mutants we examined in the present work oxidised *n*-butane to 2-butanol and propane to 2-propanol, with no evidence for the formation of the terminal alcohols. Hence, as with *n*-pentane, the bound alkanes molecules appeared to be sufficiently mobile within the active site and the ferryl intermediate oxidised the more reactive secondary C–H bonds. Unlike for *n*-pentane, however, there was no further oxidation of the secondary alcohol products to the ketones, even after the *n*-butane and propane substrates were exhausted in the reactions.

The activity trends for the smaller alkanes paralleled those for *n*-pentane. The activity was increased as the F87W, Y96F

and V247L mutations were added. The V396L mutation was detrimental to *n*-butane and propane oxidation by P450cam (Table 2), as was the F98W mutation (data not shown). The competition between the effects of the F87W and V247L mutations was again apparent, which raised the possibility that there might be changes in the structure of the enzyme when all three mutations are combined. However, the crystal structure of this triple mutant with 1,3,5-trichlorobenzene or (+)-α-pinene bound within the active site showed that the structure of both the peptide backbone and the side-chains were virtually superimposable on that of the wild-type.[53,54] Since these two substrates are more rigid and sterically demanding than the linear alkanes, it is most unlikely that the alkanes would induce structural changes. A more plausible explanation is that the F87 and V247 residues are located across the Tier 2 circle of residues (Fig. 1), such that increasing the side-chain volume at one position could push the substrate towards the other side-chain, improving the enzyme–substrate fit. However, when the side-chain volume is increased at both positions, the substrate is forced somewhere else in Tier 2, without significant improvement in activity.

The Tier 1 residues T101, L244, V295 and D297 are close to the haem.[34] We began further mutagenesis at the 295 position. It has been reported that most mutations at V295, except the V295I mutation, destabilise the P450cam protein fold.[55] When the V295I mutation was added to the F87W/Y96F/V247L triple mutant, the rate of NADH oxidation was increased slightly for both *n*-butane and propane, but crucially the coupling efficiency was lowered, especially for propane (Table 2). It is likely that the larger isoleucine side-chain at the 295 position forced the smaller propane molecule to bind away from the haem, hence the coupling was greatly reduced. In contrast, for the larger *n*-butane, the F87W/Y96F/V247L combination of mutations was more effective in holding the substrate close to the haem, thus the coupling was largely maintained.

We further investigated the possibility that the effects of the F87W and V247L mutations may be in competition with each other, by introducing the Tier 1 substitution T101L to the F87W/Y96F, Y96F/V247L and F87W/Y96F/V247L mutants. The data in Table 2 clearly show that the T101L mutation significantly increased the *n*-butane and propane oxidation rate when combined with the F87W/Y96F double mutant, but interestingly it decreased the activity when added to the Y96F/V247L mutant. Therefore, the location of the mutation added to the starting Y96F mutation is important. The T101L mutation most probably forced *n*-butane and propane to bind away from the haem in the Y96F/T101L/V247L mutant, most likely to the vicinity of the F87 side-chain which is situated directly above the 101 side-chain (Fig. 1). However, this option is not available in the F87W/Y96F/T101L mutant.

When all four mutations were combined to form the F87W/Y96F/T101L/V247L mutant, these factors and the apparently detrimental effects of the F87W/V247L combination of mutations disappeared, and the activity was the highest. These data highlight the often subtle differences between the effects of individual mutations, and especially when they are combined. Strikingly, the rate of *n*-butane oxidation by the F87W/Y96F/T101L/V247L mutant was 755 nmol per nmol of P450cam mutant per min, and with 95% coupling efficiency. This activity is 1900 times faster than that of the wild-type, and is comparable to the camphor oxidation activity of wild-type P450cam (1000 min^{-1}, >95% coupling). Hence the combined effects of the four mutations in Tiers 1 and 2 appeared to have generated an active site with near perfect fit for *n*-butane, thus shutting down the different uncoupling pathways. We note that the *n*-pentane oxidation activity of this quadruple mutant was an order of magnitude lower than that of the parent F87W/Y96F/V247L mutant (data not shown), suggesting that our strategy of reducing the active site volume to promote the oxidation of smaller alkanes may be valid. The propane oxidation rate of the F87W/Y96F/T101L/V247L mutant was 111 min^{-1}, with 32% coupling (Table 2). The 220-fold rate enhancement for propane oxidation over the wild-type was less than for *n*-butane, in all probability reflecting the need for other mutations in order to achieve the best fit for the smaller propane molecule.

The dramatic effect of the T101L mutation prompted us to introduce the T101M mutation. We found that it promoted both the NADH oxidation rate and coupling efficiency for alkane oxidation, but it was less effective than the T101L mutation (Table 2). However, it is interesting to note that the coupling for propane oxidation was in fact higher than that with the T101L mutation. Hence, analogous to the V295I mutation, the T101M mutation could prove to be effective once the NADH oxidation rate has been increased by suitable combination of mutations at other active site residues.

Finally we investigated the effect of adding bulky substitutions at the Tier 1 residues L244 and D297, to the F87W/Y96F/T101L/V247L mutant. The D297 side-chain does not contact camphor but forms a hydrogen bond to one haem propionate group (Fig. 1). The D297M mutation was introduced to probe the effect of a hydrophobic and bulky substitution at a residue close to the haem. Interestingly this mutation did not affect the stability of the protein fold even though the carboxylate side-chain of D297 forms a specific interaction with the haem prosthetic group. However, the D297M mutation reduced the *n*-butane and propane oxidation activity of the parent quadruple mutant (Table 2). In hindsight this is perhaps not so surprising because the D297 residue is quite far away from the haem iron, and even a long side-chain such as that in Met may not be sufficient to influence substrate binding and oxidation by the haem.

The side-chain of the L244 residue is already fairly bulky, and so mutations to phenylalanine and tryptophan were considered. However, the aromatic side-chains of these residues might not protrude into the active site sufficiently to promote the binding of propane. Therefore we used the L244M mutation to introduce a longer, linear side-chain. This mutation slightly reduced the *n*-butane oxidation of the F87W/Y96F/T101L/V247L mutant, but the coupling was maintained at a very high level (Table 2). Most significantly, this mutation doubled the coupling for propane oxidation, from 32 to 66%, so that the propane oxidation activity was increased to 176 min^{-1}, the highest of all the P450cam mutants studied in this work, even though the NADH oxidation activity was lowered than the parent quadruple mutant. Again we see the beneficial or potentially beneficial effects of bulky substitutions in Tier 1. This result also reinforces the need, shown by the T101M and V295I mutations, to optimise the Tier 2 mutations further so that the NADH oxidation activity is maintained while the coupling is improved by Tier 1 mutations.

The extent of uncoupling by peroxide formation

In order to provide further insight into the oxidation of *n*-butane and propane by P450cam mutants we determined the extent of uncoupling to form hydrogen peroxide for a number of mutants by a standard calorimetric assay. The data are shown in histogram form in Fig. 3. The most evident trend is that the peroxide uncoupling pathway dominates propane oxidation while *n*-butane oxidation shows much more uncoupling *via* the oxidase pathway. The Y96F/T101L/V247L mutant showed some oxidase uncoupling, but this was completely eliminated by introducing the F87W mutation to give the F87W/Y96F/T101L/V247L mutant. This observation strongly suggests that the role of the F87W mutation is to close down the top of the active site so that *n*-butane and propane are bind close to the ferryl intermediate, thus reducing uncoupling *via* the oxidase pathway.

The different effect of the T101L and T101M mutations is interesting. The T101M mutation reduced the coupling of

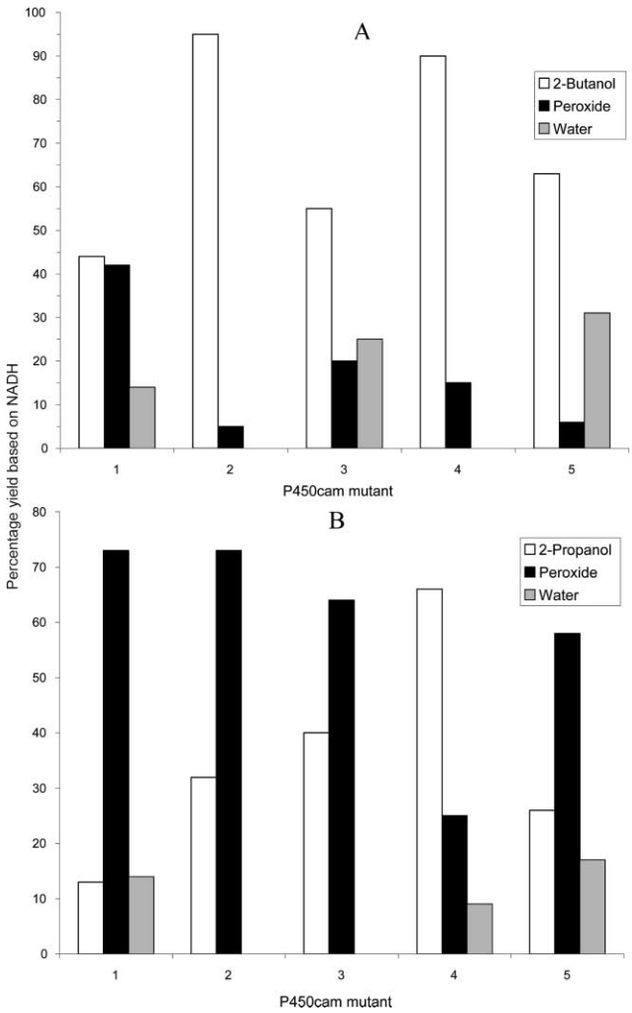

Fig. 3 The channelling of reducing equivalents from NADH to the formation of product and to the uncoupling pathways that generate hydrogen peroxide and water (oxidase pathway). (A) *n*-butane oxidation, and (B) propane oxidation. The P450cam mutants are 1: Y96F/T101L/V247L, 2: F87W/Y96F/T101L.V247L, 3: F87W/Y96F/T101M/V247L, 4: F87W/Y96F/T101L/L244M/V247L, and 5: F87W/Y96F/T101L/V247L/D297M.

n-butane oxidation by promoting the peroxide and oxidase pathway equally, while it decreased the peroxide uncoupling for propane oxidation without increasing the oxidase pathway. Hence this mutation appears to push *n*-butane away from the haem, most likely due to steric hindrance, to reduce the efficiency of substrate attack by the ferryl intermediate. With propane, however, it appears to bring the substrate closer to the haem, presumably by increasing the van der Waals interactions between the side-chain and substrate. This reduces access of water to the haem iron, *etc*., and uncoupling *via* the peroxide pathway is reduced. The D297M mutation significantly increased the uncoupling *via* the oxidase pathway. The reasons for this are not clear. The L244M mutation reduced the peroxide uncoupling for propane oxidation from 73 to 25% while increasing the oxidase pathway to 9%. The reduction of peroxide uncoupling is consistent with a reduction in active site volume and hence water access to the haem iron. The slight increase in oxidase uncoupling suggests a longer average distance of the substrate from the ferryl intermediate and supports the need for further engineering near the top of the active site to constrain propane to bind closer to the haem.

Ethane and methane

None of the P450cam mutants showed any significant activity for the oxidation of ethane and methane even though the most active mutants for *n*-butane and propane oxidation had NADH oxidation rates as high as *ca*. 50 min^{-1} under atmospheric pressure. The reactions are clearly slow and almost totally uncoupled, indicating that there is still some way to go before these smallest of alkanes can be bound sufficiently close to the haem to lead to fast NADH oxidation with good coupling to product formation. Reactions were also carried out at 10 atm partial pressures of both the alkane and oxygen. We were not able to monitor the NADH oxidation rates in these reactions, but no products were detected.

Summary and conclusions

We have shown conclusively that cytochrome P450cam can be engineered to an alkane hydroxylase, with activities that can approach that for the oxidation of the natural substrate, camphor. The enzyme was successfully engineered for the oxidation of *n*-butane and propane by the approach of improving the enzyme/substrate fit *via* reduction of the active site volume. We first introduced substitutions with amino acids with bulky side-chains at residues located higher up in the active site, and then used similar substitutions at residues close to the haem. The results also suggest a number of other additional mutations that could further increase the activity. However, some of the mutations at certain sites had unpredictable consequences. Moreover, even the most active mutants for propane oxidation did not oxidise ethane or methane, and further protein engineering is required for these, the smallest alkanes. Since all the alkanes are oxidised at the secondary carbon positions, these substrates remain mobile, at least conformationally, within the active site. Therefore it appears that it is relatively straightforward to engineer a P450 enzyme to oxidise an unnatural substrate with high activity and coupling, but manipulating the binding orientation and hence product selectivity is a more difficult problem, especially for flexible molecules.

Acknowledgements

This work was supported by the Biotechnology and Biological Sciences Research Council and the Engineering and Physical Sciences Research Council (EPSRC), UK, under grant B10666. J.-A. S. was supported by a studentship from the EPSRC. We also thank the referees for helpful comments and suggestions.

References

1 F. P. Guengerich, *J. Biol. Chem.*, 1991, **266**, 10019.
2 P. R. Ortiz de Montellano, in *Cytochrome P450: Structure, Mechanism and Biochemistry*, Plenum, New York, 1995.
3 E. J. Mueller, P. J. Loida and S. G. Sligar, in *Cytochrome P450: Structure, Mechanism and Biochemistry*, ed. P. R. Ortiz de Montellano, Plenum, New York, 1995.
4 J. T. Groves and Y.-Z. Han, in *Cytochrome P-450: Structure, Mechanism and Biochemistry*, ed. P. R. Ortiz de Montellano, Plenum, New York, 1995.
5 D. G. Kellner, S. A. Maves and S. G. Sligar, *Curr. Opin. Biotechnol.*, 1997, **8**, 274.
6 L. L. Wong, *Curr. Opin. Chem. Biol.*, 1998, **2**, 263.
7 C. S. Miles, T. W. Ost, M. A. Noble, A. W. Munro and S. K. Chapman, *Biochim. Biophys. Acta*, 2000, **1543**, 383.
8 I. C. Gunsalus and G. C. Wagner, *Methods Enzymol.*, 1978, **52**, 166.
9 L. O. Narhi and A. J. Fulco, *J. Biol. Chem.*, 1986, **261**, 7160.
10 Y. Miura and A. J. Fulco, *Biochim. Biophys. Acta*, 1975, **388**, 305.
11 S. S. Boddupalli, B. C. Pramanik, C. A. Slaughter, R. W. Estabrook and J. A. Peterson, *Arch. Biochem. Biophys.*, 1992, **292**, 20.
12 T. Zimmer, T. Iida, W. H. Schunck, Y. Yoshida, A. Ohta and M. Takagi, *Biochem. Biophys. Res. Commun.*, 1998, **251**, 244.
13 A. Bosetti, J. B. Van Beilen, H. Preusting, R. G. Lageveen and B. Witholt, *Enzyme Microb. Technol.*, 1992, **14**, 702.
14 J. B. van Beilen, J. Kingma and B. Witholt, *Enzyme Microb. Technol.*, 1994, **16**, 904.
15 I. E. Staijen, J. B. Van Beilen and B. Witholt, *Eur. J. Biochem.*, 2000, **267**, 1957.
16 J. Colby, D. I. Stirling and H. Dalton, *Biochem. J.*, 1977, **165**, 395.
17 H. Dalton, *Adv. Appl. Microbiol.*, 1980, **26**, 71.

18 J. Green and H. Dalton, *J. Biol. Chem.*, 1989, **264**, 17698.
19 S. J. Pilkington and H. Dalton, *Methods Enzymol.*, 1990, **188**, 181.
20 G. M. Tonge, D. E. Harrison and I. J. Higgins, *Biochem. J.*, 1977, **161**, 333.
21 J. D. Lipscomb, *Annu. Rev. Microbiol.*, 1994, **48**, 371.
22 B. G. Fox, W. A. Froland, J. E. Dege and J. D. Lipscomb, *J. Biol. Chem.*, 1989, **264**, 10023.
23 J.-A. Stevenson, A. C. G. Westlake, C. Whittock and L.-L. Wong, *J. Am. Chem. Soc.*, 1996, **118**, 12846.
24 J.-A. Stevenson, J. K. Bearpark and L.-L. Wong, *New J. Chem.*, 1998, 551.
25 S. G. Bell, J.-A. Stevenson, H. D. Boyd, S. Campbell, A. D. Riddle, E. L. Orton and L.-L. Wong, *Chem. Commun.*, 2002, 490.
26 A. Glieder, E. T. Farinas and F. H. Arnold, *Nat. Biotechnol.*, 2002, **20**, 1135.
27 C. F. Harford-Cross, A. B. Carmichael, F. K. Allan, P. A. England, D. A. Rouch and L.-L. Wong, *Prot. Eng.*, 2000, **13**, 121.
28 D. P. Nickerson, C. F. Harford-Cross, S. R. Fulcher and L. L. Wong, *FEBS Lett.*, 1997, **405**, 153.
29 J. P. Jones, E. J. O'Hare and L. L. Wong, *Chem. Commun.*, 2000, 247.
30 J. P. Jones, E. J. O'Hare and L. L. Wong, *Eur. J. Biochem.*, 2001, **268**, 1460.
31 S. G. Bell, R. J. Sowden and L.-L. Wong, *Chem. Commun.*, 2001, 635.
32 J. A. Fruetel, J. R. Collins, D. L. Camper, G. H. Loew and P. R. Ortiz de Montellano, *J. Am. Chem. Soc.*, 1992, **114**, 6987.
33 D. Filipovic, M. D. Paulsen, P. J. Loida, S. G. Sligar and R. L. Ornstein, *Biochem. Biophys. Res. Commun.*, 1992, **189**, 488.
34 P. J. Loida and S. G. Sligar, *Biochemistry*, 1993, **32**, 11530.
35 O. Sibbesen, Z. Zhang and P. R. Ortiz de Montellano, *Arch. Biochem. Biophys.*, 1998, **353**, 285.
36 D. A. Grayson, Y. B. Tewari, M. P. Mayhew, V. L. Vilker and R. N. Goldberg, *Arch. Biochem. Biophys.*, 1996, **332**, 239.
37 M. P. Mayhew, A. E. Roitberg, Y. Tewari, M. J. Holden, D. J. Vanderah and V. L. Vilker, *New J. Chem.*, 2002, **26**, 35.
38 K. J. French, M. D. Strickler, D. A. Rock, G. A. Bennett, J. L. Wahlstrom, B. M. Goldstein and J. P. Jones, *Biochemistry*, 2001, **40**, 9532.
39 K. J. French, D. A. Rock, J. I. Manchester, B. M. Goldstein and J. P. Jones, *Arch. Biochem. Biophys.*, 2002, **398**, 188.
40 J. Sambrook, E. F. Fritsch and T. Maniatis, *Molecular Cloning: A Laboratory Manual*, Cold Spring Harbor Laboratory Press, New York, 1989.
41 A. C. Westlake, C. F. Harford-Cross, J. Donovan and L. L. Wong, *Eur. J. Biochem.*, 1999, **265**, 929.
42 J. A. Peterson, M. C. Lorence and B. Amarneh, *J. Biol. Chem.*, 1990, **265**, 6066.
43 T. Yasukochi, O. Okada, T. Hara, Y. Sagara, K. Sekimizu and T. Horiuchi, *Biochim. Biophys. Acta*, 1994, **1204**, 84.
44 D. P. Nickerson and L.-L. Wong, *Prot. Eng.*, 1997, **10**, 1357.
45 T. L. Poulos, B. C. Finzel and A. J. Howard, *J. Mol. Biol.*, 1987, **195**, 687.
46 W. M. Atkins and S. G. Sligar, *J. Biol. Chem.*, 1988, **263**, 18842.
47 R. A. Marcus and N. Sutin, *Biochim. Biophys. Acta*, 1985, **811**, 265.
48 M. J. Honeychurch, H. A. O. Hill and L. L. Wong, *FEBS Lett.*, 1999, **451**, 351.
49 R. Raag and T. L. Poulos, *Biochemistry*, 1991, **30**, 2674.
50 R. Raag and T. L. Poulos, *Biochemistry*, 1989, **28**, 917.
51 R. Raag and T. L. Poulos, *Biochemistry*, 1989, **28**, 7586.
52 T. L. Poulos, B. C. Finzel and A. J. Howard, *Biochemistry*, 1986, **25**, 5314.
53 X. Chen, A. Christopher, J. P. Jones, S. G. Bell, Q. Guo, F. Xu, Z. Rao and L. L. Wong, *J. Biol. Chem.*, 2002, **277**, 37519.
54 S. G. Bell, X. Chen, R. J. Sowden, F. Xu, J. N. Williams, L. L. Wong and Z. Rao, *J. Am. Chem. Soc.*, 2003, **125**, 705.
55 S. G. Sligar, D. Filipovic and P. S. Stayton, *Methods Enzymol.*, 1991, **206**, 31.